

**FY2020 FES Theory Milestone**  
**“Modeling of Fully 3D Vertical Displacement Event Disruptions”**

**Final Report – September 30, 2020**

**DRAFT**

**Prepared by: S. C. Jardin, C. Clauser, *PPPL*; C. Sovinec, *U. Wisconsin-Madison***

**Summary:** This is the final report detailing the successful completion of the FY2020 FES Theory Milestone. This builds on the progress reported in the three quarterly reports already submitted; **Q1:** Perform and document benchmark M3D-C1/NIMROD 2D VDE calculations in simplified geometry; **Q2:** Perform several 2D VDE simulations of ITER using either NIMROD or M3D-C1 with differing “halo current” parameters to determine likely worst case configurations regarding axisymmetric vessel forces; **Q3:** Perform and document benchmark M3D-C1/NIMROD 3D VDE calculations in simplified geometry. To these, we add successful completion of the final quarterly milestone: **Q4:** Complete a 3D VDE simulation of ITER using either NIMROD or M3D-C1 with “worst case” halo parameters (as determined in Q2) to determine the magnitude of the sideways force.

## **1. Introduction**

Vertical Displacement Events (VDEs) are major disruption events in tokamaks. They occur when the vertical stability control is lost and the entire plasma column moves up or down, hitting the wall and disrupting. These events produce large current densities in the wall due to both induction from the plasma motion and current quench, and due to halo currents shared by the plasma and the wall. The  $\mathbf{J} \times \mathbf{B}$  forces due to these currents will produce large forces that potentially can damage the vessel. A good understanding of these forces is required for several reasons: (i) to gain confidence and secure approvals during initial operation in order to increase the plasma current and toroidal field to the full design values, and (ii) to evaluate and employ effective mitigation techniques to minimize stresses on the components.

The forces that develop during the VDE and the associated modeling of these forces can be divided into two categories; symmetrical and asymmetrical. Symmetrical VDE forces are those that arise when the plasma motion and associated vessel currents are independent of the toroidal angle  $\varphi$ . These have been extensively modeled by 2D (axisymmetric) codes and were the subject of our Q2 progress report and the associated publication [1] and are primarily in the vertical direction.

This final theory milestone is primarily concerned with asymmetrical VDEs, or AVDEs. Asymmetrical vessel forces, sometimes called horizontal forces or “sideways forces”, arise from 3D kinking motions of the plasma, usually during the late stages of the event. These plasma motions can induce and conduct 3D current patterns into the surrounding vessel which interact with the toroidal field to produce asymmetrical forces. Previous papers predict large values for these forces in ITER. These predictions

were obtained by scaling results from present tokamaks [2], by performing calculations with increased wall resistivity and scaling the results to those of ITER [3,4], or by analytic estimates [5-7].

The goal of the present work, and the associated milestone, is to calculate these sideways forces directly from a 3D MHD simulation using realistic values for the wall resistivity in ITER. The present focus is on M3D-C1 simulations, although it was shown in the Q3 report that NIMROD simulations will provide results in quantitative agreement with those of M3D-C1 when modeling AVDEs.

This paper is organized as follows: Section 2 describes our initial calculations using a pre-existing model of the ITER vessel with the conducting structure at the first wall [1] as used in the Q2 report. Section 3 presents an improved vessel model in which the wall resistivity a function of space and with different values for the poloidal and toroidal resistivities in the wall. Section 4 presents a discussion of the wall forces calculated, and what may be the reason that they differ from those obtained by a straightforward scaling of results in existing tokamaks. Section 5 provides a short summary and suggestions for future work.

## 2. Results with preliminary vessel model

The initial model we used for the ITER vessel was that used in the Q2 report and shown in Fig. 1, frames (A) and (F). We represent the ITER vessel as a 6-cm thick conducting structure located at the first wall.

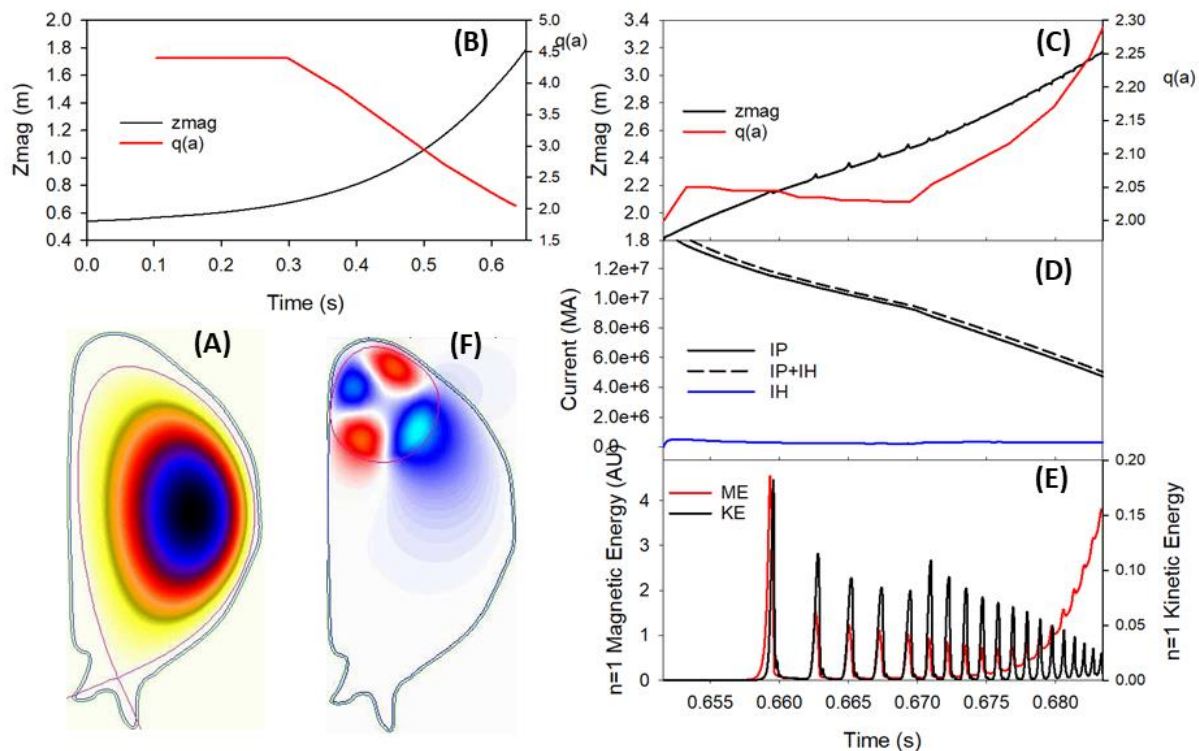
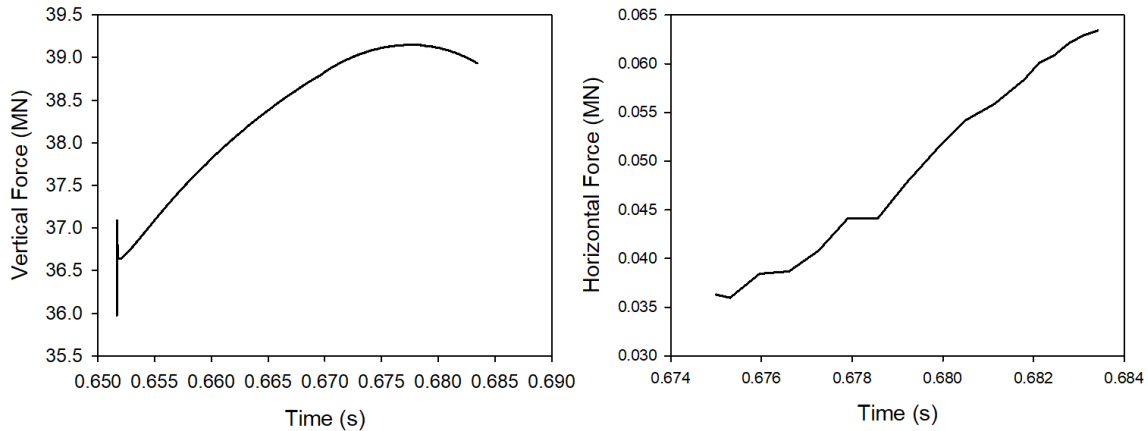


Figure 1 (A) Contours of plasma current density at start of 2D calculation; (B) Position of the magnetic axis and value of edge safety factor during the 2D phase of the calculation; (C) Position of the magnetic axis and value of the edge safety factor during the 3D phase of the calculation; (D) Plasma current and Halo current during the 3D phase; (E) Energy in the  $n=1$

toroidal harmonic of the magnetic field and kinetic energy during the 3D phase; (F) Contours of the toroidal derivative of the poloidal flux at the end of the 3D phase, showing a (2,1) mode structure.

The wall resistivity was chosen so that the vessel would have a  $L/R$  time of 235 ms, the same resistivity as used in Ref. [1]. We started the calculation in 2D, assuming axisymmetry, as was done in Ref. [1]. Plotted in Fig. 1B is the position of the magnetic axis and the value of the edge safety factor,  $q(a)$ , as a function of time. At time  $t=0.6516$  s, when  $q(a)=2$ , the calculation was switched to 3D and the isotropic thermal conductivity was increased from  $1.e-6$  to  $0.05$  to simulate the effect of fine scale surface breakup caused by the thermal quench. The plasma  $\beta$  immediately dropped from  $5.e-3$  to  $2.5e-5$  and the central temperature dropped to about 30 eV. Figure 1C shows the magnetic axis position and the  $q(a)$  evolution during the 3D phase. Figure 1D shows the plasma and halo currents vs time, and Fig. 1E shows the  $n=1$  component of the energies in the magnetic field and kinetic energy during the 3D phases. These energies are seen to occur in quasi-periodic bursts with the amplitude and the time between bursts generally decreasing in time. The exception is that at about time  $t=0.675$  s the  $n=1$  magnetic energy monotonically rises for 10 ms at which time the calculation was terminated. In Fig. 1F we plot the toroidal derivative of the poloidal magnetic flux at the final time. We see there is a dominant (2,1) mode present.



**Figure 2** Forces on the vessel vs time for all (left) or part (right) of the 3D phase of the calculation. On the left is the vertical force. On the right is the horizontal force.

The net vertical and horizontal forces on the vessel are shown in Figure 2 as a function of time. The maximum vertical force of about 40 MN is consistent with that found in the 2D calculations described in the Q2 report and in Ref. [1]. At 0.065 MN, the maximum horizontal force is much smaller than the vertical force. We suspect that the horizontal force is lower than expected from a simple scaling of the results from JET [2] for at least two reasons. One is that we see in Figure 1C that the value of  $q(a)$  is actually increasing in time during the 3D phase. This leads to increased  $n > 0$  stability, and presumably to decreased wall forces. The other is that the close fitting conducting wall used in this calculation is very stabilizing. This led to the improved vessel model described in the next section.

To test the sensitivity of this result to the halo current fraction, we chose a companion 2D case from Ref. [1] with a larger halo fraction from which to launch a 3D case with otherwise very similar parameters to

those used here. We found that the horizontal force in the large halo fraction case, with 30% halo fraction, was actually consistently lower than the horizontal force in the calculation presented here, with only 6% halo fraction.

### 3. An improved vessel model

We suspected that the reason the horizontal force was so small in the calculation described in Sec. 2 was because the conducting structure was so close to the plasma. In reality, the 6 cm thick conducting structure is located behind the blanket modules, about 60 cm away from the first wall, and there are a series of supports connecting the plasma facing component with the conducting structure. The actual structure is too complex to represent in M3D-C1 in detail, but we have developed an improved vessel model that we show in Fig. 3.

The “new” vessel model shown in Fig. 3 has two regions. The thick region, closest to the plasma, has different resistivities in the poloidal and toroidal directions. The poloidal resistivity is very low,  $\eta_p = 1.0 \text{ E-6 } \Omega\text{-m}$ , allowing halo currents to easily flow to the outer conducting structure. However, the toroidal resistivity is very high,  $\eta_T = 1.0 \text{ E-2 } \Omega\text{-m}$ , preventing substantial stabilizing toroidal currents from appearing in this region. Because the region with good toroidal conductivity is further away from the plasma in the new structure, compared with the old structure, we can expect that the VDE growth time will be shorter, and that the vessel will also be less stabilizing to the MHD  $n > 0$  modes.

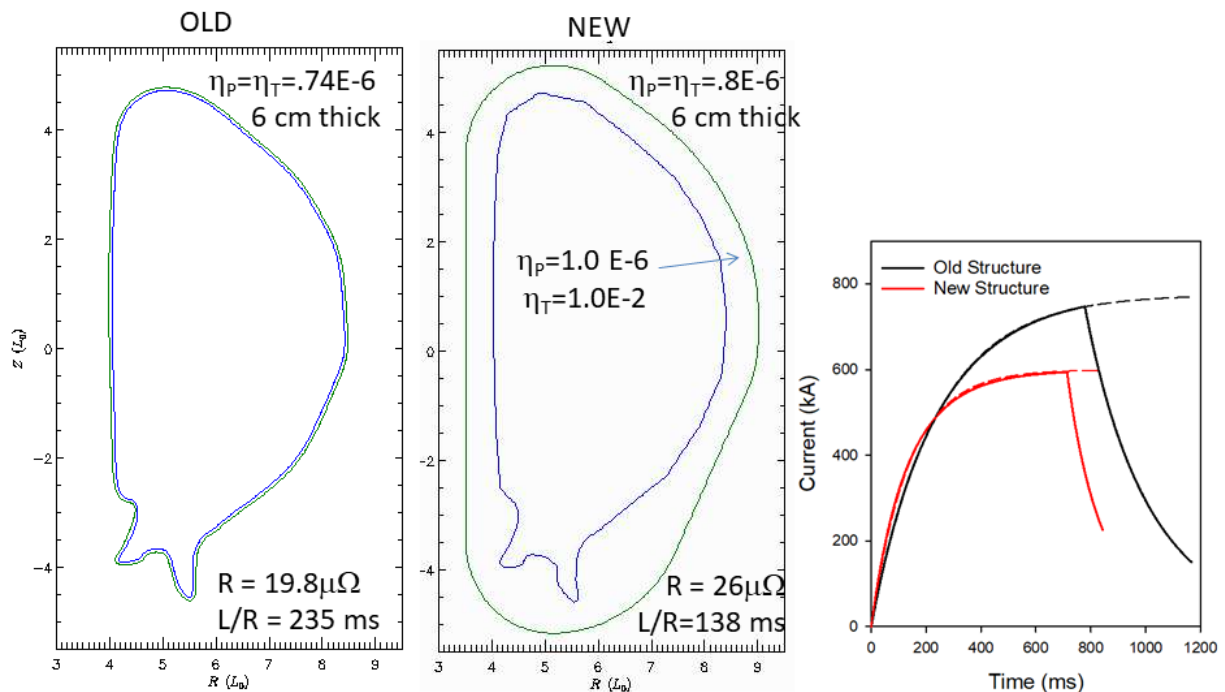


**Figure 3:** Left is a diagram of the "old" vessel model used in Section 2. Center is the new vessel model with anisotropic resistivity in the structure. Right is a comparison of the responses to a step loop voltage.

Calculations were performed with this new vessel model and are summarized in Figure 4. The calculation was initiated in 2D (axisymmetric) as shown in Figures 4A and 4B. Figure 4A shows the Z-

position of the magnetic axis and the edge safety factor as a function of time. Figure 4B shows the plasma current,  $I_P$ , and the plasma  $\beta$  as a function of time. We use this 2D calculation to initiate full 3D calculations at three different values of the edge  $q$ : (b)  $q(a) = 1.7$ , (c)  $q(a) = 1.2$ , and (d)  $q(a) = 0.9$ .

The full 3D evolution of the three runs, with different initial conditions and different starting times are plotted in Fig. 4 frames C-F. The times in the horizontal axis are time in ms since the start of the 3D calculation. Figure 4C shows the energy in the  $n=1$  toroidal component of the magnetic field, Figure 4D shows the corresponding growth rate, and Fig. 4E shows the horizontal, or sideways, force for each of the 3 cases. Although the horizontal force of case (d) is over 5 times large than that shown in Fig. 2 for the original structure model, it is still small compared to values expected from a straightforward extrapolation of JET experimental results [2].

In Fig. 4F we plot the mode structure for each of the three runs at the time of maximum amplitude for each run. We plot the toroidal derivative of the electrostatic potential, which is closely related to the toroidal derivative of the velocity stream function for the poloidal flow. All of the cases have the

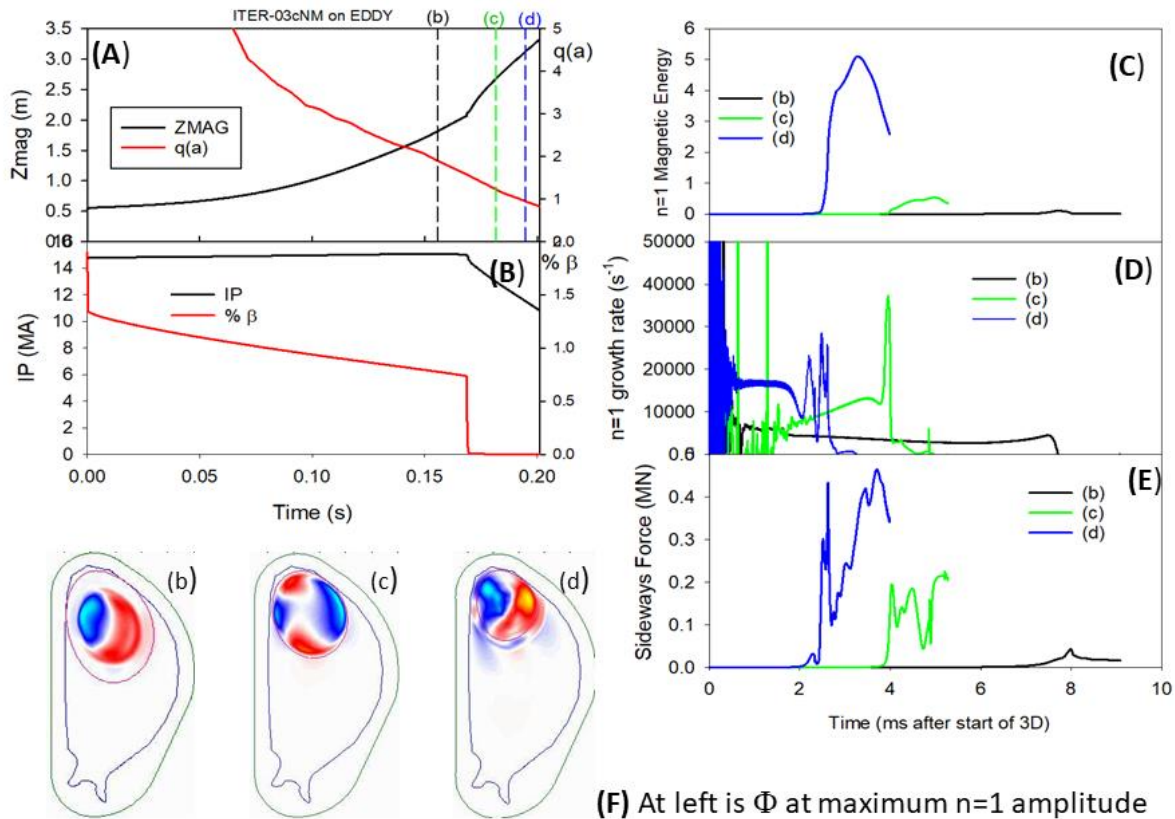


**Figure 4: Summary of calculations with new vessel model. Figures (A) and (B) are of a 2D (axisymmetric) calculation. (A) shows the z-position of the magnetic axis and the edge safety-factor  $q(a)$  as a function of time. (B) shows the plasma current and  $\beta$  as a function of time. We use this run to initiate three 3D runs that start at different times in the 2D run. 3D run (b) starts with  $q(a) = 1.7$ , run (c) starts with  $q(a) = 1.2$ , and run(d) starts with  $q(a)=0.9$ . Shown in (C) is the magnetic energy in the  $n=1$  harmonic for the 3 runs vs time. Figure (D) shows the corresponding growth rates as a function of time, and (E) shows the horizontal, or sideways force, as a function of time. In Figure (F) we plot the toroidal derivative of the electrostatic potential for the 3 runs, each at the time when the  $n=1$  amplitude, Figure (E), is at the maximum value.**

toroidal  $n=1$  mode dominant. In case (b), we see that the poloidal mode structure is dominantly  $m=1$ , but it is an internal mode. Case (c) has a dominant  $m=2$  external mode, and case (d) has a dominant  $m=1$  external mode.

#### 4. Discussion

The horizontal forces plotted in Figs. 2 and 4E are still small compared to those obtained by straightforward extrapolation of JET experimental results [2]. The reason for this may be the fact that the ITER vessel is a very good conductor compared to the vacuum vessels of existing tokamaks.

Strauss performed a series of idealized AVDE calculations in which he varied the resistivity of the vessel but kept the plasma parameters the same. He found the result that the sideways wall force was a maximum at an intermediate value of the wall resistivity. In his runs, if the plasma was unstable to a mode with growth rate  $\gamma$  and the wall had a resistive time  $\tau_w$ , he found that the horizontal force was a maximum when  $\gamma \tau_w \sim 1$  [8]. This is a potentially important result, but it cannot immediately be extrapolated to ITER conditions since the wall time in the Strauss calculation was comparable to the Alfvén time, and the entire calculation was only for about 50 Alfvén times. In contrast, the ITER wall time is  $10^5$  or  $10^6$  Alfvén times.

The Strauss result, that the wall forces are a maximum at an intermediate value of  $\gamma \tau_w$  got a boost from a 2015 paper by Pustovitov [9]. In this paper, he showed that in general, the net force on the wall could be computed by performing the following integral *exterior* to the vacuum vessel:

$$\mathbf{u} \cdot \mathbf{F}_w = \mathbf{u} \cdot \int_{wall} \mathbf{j} \times \mathbf{B} dV = \oint_{wall+} \left[ (\mathbf{u} \cdot \mathbf{B}) \mathbf{B} - \frac{B^2}{2} \mathbf{u} \right] \cdot d\mathbf{S} \quad (1)$$

Here,  $\mathbf{u}$  is any constant vector, such as a unit vector in the x-direction. The fact that this integral is exterior to the vessel implies that the force vanishes in the limit  $\gamma \tau_w \rightarrow \infty$  (ideal wall) as well as in the limit  $\gamma \tau_w \rightarrow 0$  (no mode or induced current). While this result, that the force is a maximum at an intermediate value of  $\gamma \tau_w$ , is qualitatively in agreement with the Strauss result, it does not predict for which value of  $\gamma \tau_w$  the maximum will occur, or what it will be.

#### 5. Summary and Future Work

This report describes the first ever 3D MHD simulation of a vertical displacement event disruption in ITER using a model for the ITER vacuum vessel with a realistic time constant and a multi-region conductivity model. The vertical vessel forces that we calculate are consistent with those obtained previously with 2D simulations [1]. The horizontal (or sideways) forces calculated are substantially smaller than what one would obtain from a straightforward scaling of JET results to larger values of the plasma current and magnetic field. We hypothesize that this is due to the fact that the ITER vessel is a much better electrical conductor than is the JET vessel. However, this needs to be demonstrated by redoing this calculation with a (unrealistic) high-resistivity vessel to see if we get much larger forces. Also, the model we use in Section 3, while a substantial improvement over that used in Section 2, is still

considerably simplified compared to the actual ITER vessel, and it would be prudent to redo the calculations presented here with an even more realistic vessel model. This would require some code modifications and would likely use considerably more computer resources.

## Acknowledgements

This work was supported by U.S. DOE Contract Nos. DE-AC02-09CH11466 and DE-SC0018001 and the SciDAC Center for Tokamak Transient Simulations. The computations presented in this report used resources of the National Energy Research Scientific Computing Center (NERSC), a U.S. Department of Energy Office of Science User Facility operated under Contract No. DE-AC02-05CH11231.

## Appendix: Benchmark of multi-region poloidal resistivity structure

As part of the new M3D-C1 structure model described in Section 3, we added the capability of having a structure with different poloidal and toroidal resistivities, and those resistivities could be functions of space within the conductor. To accommodate the different poloidal and toroidal vessel resistivities, we modified the finite element equations for the time derivative of the poloidal flux and toroidal field as follows:

$$\frac{1}{R^2}(v_i, \dot{\psi}) = -\frac{\eta_T}{R^2} \Delta^* v_i \Delta^* \psi + \frac{\eta_P}{R^2} \left[ \frac{1}{R^2}(v_i, \psi'') + [v_i, f'''] + [v_i, F'] \right] + \frac{\eta'_P}{R^2} \left[ \frac{1}{R^2}(v_i, \psi') + [v_i, f''] + [v_i, F] \right] \quad (\text{A1})$$

$$\frac{v_i}{R^2} \dot{F} = -\frac{\eta_P}{R^2}(v_i, F) - \frac{\eta_P}{R^2}(v_i, f'') + \frac{\eta_P}{R^2}[v_i, \psi'] \quad (\text{A2})$$

The notation used here for the magnetic field variables, the inner and vector products, and the finite element basis functions is the same as used in Ref. [10]. The difference is that the scalar wall resistivity in Ref. [10] is replaced the toroidal or poloidal wall resistivities,  $\eta_T$  or  $\eta_P$ .

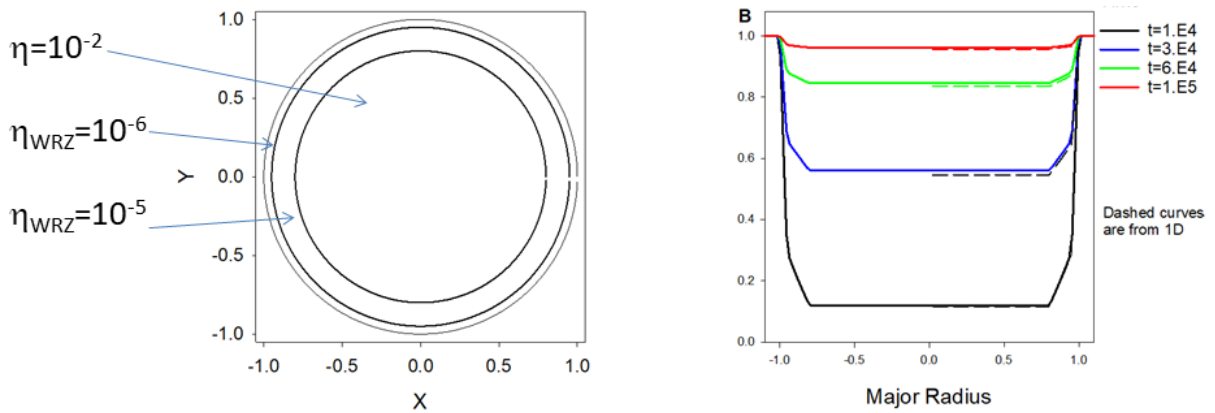


Figure A1: 1D test problem for varying wall poloidal resistivity. Left shows 1D geometry used. Right shows a comparison of the magnetic field vs major radius at 4 different times

To test the multi-region poloidal resistivity model, we set up a test problem as shown in Figure A1. On the left is the 1D multi-region geometry used. On the right is a comparison of the results from the 1D code and the M3D-C1 calculation. Solid is the M3D-C1 solution and dotted is the solution from the separate 1D code. As boundary conditions, a poloidal loop voltage was applied at the boundary, ramping up from 0 to 1 V in  $10^4 \tau_A$  and then held constant. We see that the agreement is excellent, thus verifying the M3D-C1 model.

## References:

- [1] C. F. Clauser, S. C. Jardin, and N. M. Ferraro, Nucl. Fusion **59** (2019) 126037
- [2] L.E. Zakharov, S. A. Galkin, S. N. Gerasimov, Phys. Plasmas **19** (2012) 055703
- [3] H. Strauss, et al, Phys. Plasmas **17** (2010) 082505
- [4] H. Strauss, Phys. Plasmas **27** (2020) 022508
- [5] D. V. Mironov and V.D. Pustovitov, Phys. Plasmas **22** (2015) 052502
- [6] D. V. Mironov and V. D. Pustovitov, Phys. Plasmas **24** (2020) 092508
- [7] A. A. Martynov and S.Y. Medvedev, Phys. Plasmas **27** (2020) 012508
- [8] H. Strauss, R. Paccagnella, and J. Breslau, Phys. Plasmas **17**, 082505 (2010)
- [9] V. D. Pustovitov, Nucl. Fusion **55** 113032
- [10] J. Breslau, N. Ferraro, S. Jardin, Phys. Plasmas, **16** 092503 (2009)